Extended Trench Gate Superjunction Lateral Power MOSFET for Ultra-Low Specific on-Resistance and High Breakdown Voltage

Doohyung Cho and Kwangsoo Kim

In this paper, a lateral power metal–oxide–semiconductor field-effect transistor with ultra-low specific on-resistance is proposed to be applied to a high-voltage (up to 200 V) integrated chip. The proposed structure has two characteristics. Firstly, a high level of drift doping concentration can be kept because a tilt-implanted p-drift layer assists in the full depletion of the n-drift region. Secondly, charge imbalance is avoided by an extended trench gate, which suppresses the trench corner effect occurring in the n-drift region and helps achieve a high breakdown voltage (BV). Compared to a conventional trench gate, the simulation result shows a 37.5% decrease in $R_{on.sp}$ and a 16% improvement in BV.

Keywords: Superjunction, power MOSFET, LD-MOSFET, breakdown, on-resistance.

Manuscript received Aug. 21, 2013; revised Mar. 15, 2014; accepted Mar. 28, 2014.

This research was supported by the MSIP (Ministry of Science, ICT and Future Planning), Korea, under the ITRC (Information Technology Research Center) support program (NIPA-2014-H0301-14-1007) supervised by the NIPA (National IT Industry Promotion Agency).

Doohyung Cho (corresponding author, doohyung@sogang.ac.kr) and Kwangsoo Kim (kimks@sogang.ac.kr) are with the Department of Electronic Engineering, Sogang University, Seoul, Rep. of Korea.

I. Introduction

The development of high-voltage lateral power metal–oxide–semiconductor field-effect transistors (MOSFETs) has been limited due to high specific on-resistance caused by a relatively long drift region. To overcome this demerit, a conventional trench gate (CTG)-LDMOSFET (see Fig. 1(a)) using thick oxide and a trench gate has been proposed; however, a CTG-LDMOSFET is optimized for low-voltage applications due to its low breakdown voltage (BV) [1]–[4]. More specifically, use of a CTG-LDMOSFET in such applications increases the likelihood of a premature breakdown — caused by electric field crowding occurring at the bottom corners of the trench gate [5]. To solve the trench corner effect so that CTG-LDMOSFETs can be used in high-voltage applications, an extended trench gate (ETG) structure (see Fig. 1(b)) is proposed [6].

The ETG structure suppresses the trench corner effect by extending the trench gate to the p-substrate. The ETG helps to achieve a more uniform electric field distribution and extend the on-state channel electron accumulation in the n-drift region to elevate the current density. Consequently, an improvement in both BV and $R_{on.sp}$ (specific on-resistance), compared to a CTG, is obtained [6]. To sustain high voltages, CTG and ETG structures require low levels of n-drift doping concentration as well as increases to both cell pitch and the size of thick oxide used. However, such requirements increase $R_{on.sp}$; thus, a technique for achieving low $R_{on.sp}$ is needed. Therefore, an extended trench gate superjunction (ETGSJ)-LDMOSFET with a high BV and low $R_{on.sp}$ is proposed.

© 2014 ETRI

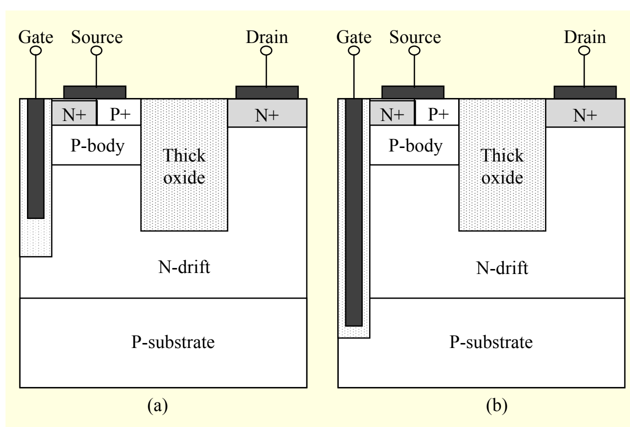

Fig. 1. Schematic cross sections of (a) CTG [4] and (b) ETG [6].

We will explain the proposed ETGSJ LDMOSFET structure in Section II. In Section III, we explain the optimization of device parameters through the use of a simulation tool and analyze the electrical characteristics of the ETGSJ structure. Lastly, Section IV concludes the paper.

II. Proposed Device Structure

A cross-sectional view of the proposed ETGSJ structure is shown in Fig. 2. Here, the thick oxide helps to improve the reduced surface field (RESURF) by allowing multiple directional depletion. In addition, the lateral-direction electric field decreases due to the low permittivity of the oxide [6]–[7]. Meanwhile, due to the drift charge-balance effect, electric field modulation in the drift region occurs; this in turn, results in the creation of a uniform electric field. Therefore, a higher BV can be obtained in the ETGSJ structure compared to that obtained in a CTG or ETG structure. To obtain a higher BV, CTG and ETG structures must be able to tolerate increases to both cell pitch and the size of thick oxide used. However, an increase in the size of thick oxide used causes a narrowing of the path of the current in the n-drift region. Subsequently, this causes an increase in $R_{on.sp}$. Conversely, increases in cell pitch widen the path of the current. Therefore, the level of n-drift doping concentration should be lowered to achieve full depletion of the n-drift region. As the proposed ETGSJ structure can fully deplete the drift region, through the use of a charge balance effect and drift doping concentration control [8], a uniform electric field distribution can be achieved while simultaneously maintaining a high level of drift doping concentration. In addition, the ETGSJ structure can easily be applied to high-voltage applications. This is because the drift depletion width in the respective drift region can be controlled to cope with variations in cell pitch. As a result, the proposed ETGSJ structure owes its improvement of performance to the following three characteristics: firstly, the operation of the charge balance effect in the drift region — this results in a more uniform electric field, which in turn gives rise to a higher BV; secondly, the use of junction depletion — the whole structure can be fully depleted while maintaining a relatively high level of drift doping concentration; and lastly, the increased depth of the trench gate — this helps avoid charge imbalances and affords the use of high-density currents.

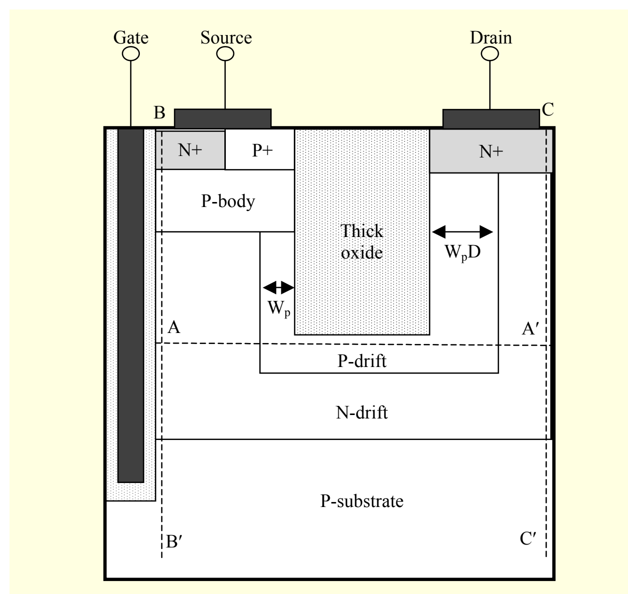

Fig. 2. Schematic cross-section of proposed ETGSJ structure.

III. Simulation Result and Discussion

For the evaluation of electrical characteristics and its optimization of the proposed structure, the 2D device simulator ATLAS is used [9]. The epitaxial layer of the ETGSJ structure is grown on the p-substrate (1×10^{15} cm^{-3}) to a thickness of 6 μm. In addition, it is designed and optimized with N_D/N_A drift doping concentration (1×10^{16} cm^{-3}) and thick oxide (width = 3.5 μm and depth = 4 μm). Charge imbalance occurs with the help of an asymmetric charge component in the drift region. It is necessary to find the optimal widths of W_p and W_pD as well as the optimum level of doping concentration, because the asymmetric charge component in the drift region decreases the depletion width of the drift region, which in turn causes premature breakdown. Consequently, simulations are necessary to determine these optimal values, which, once determined, will help to minimize the charge-imbalance effect [10]. For an exact performance comparison across the three structures (CTG, ETG, and ETGSJ), the value of each respective parameter, except for the level of the drift doping concentration in the ETGSJ structure, is kept the same across the three structures.

http://dx.doi.org/10.4218/etrij.14.0113.0826

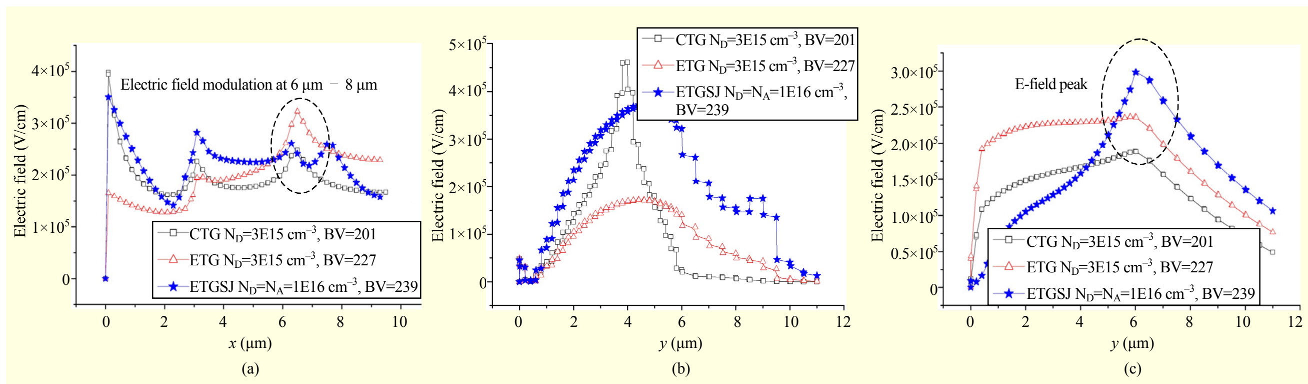

Fig. 3. Electric field distributions (at breakdown for the three different structures) in the (a) lateral direction (y = –1.9, cross section: A-A′) along the thick oxide bottom, (b) vertical direction (x = 0.51, cross section: B-B′) along the sidewall of the trench gate, and (c) vertical direction (x = 9.9, cross section: C-C′) along the drain region.

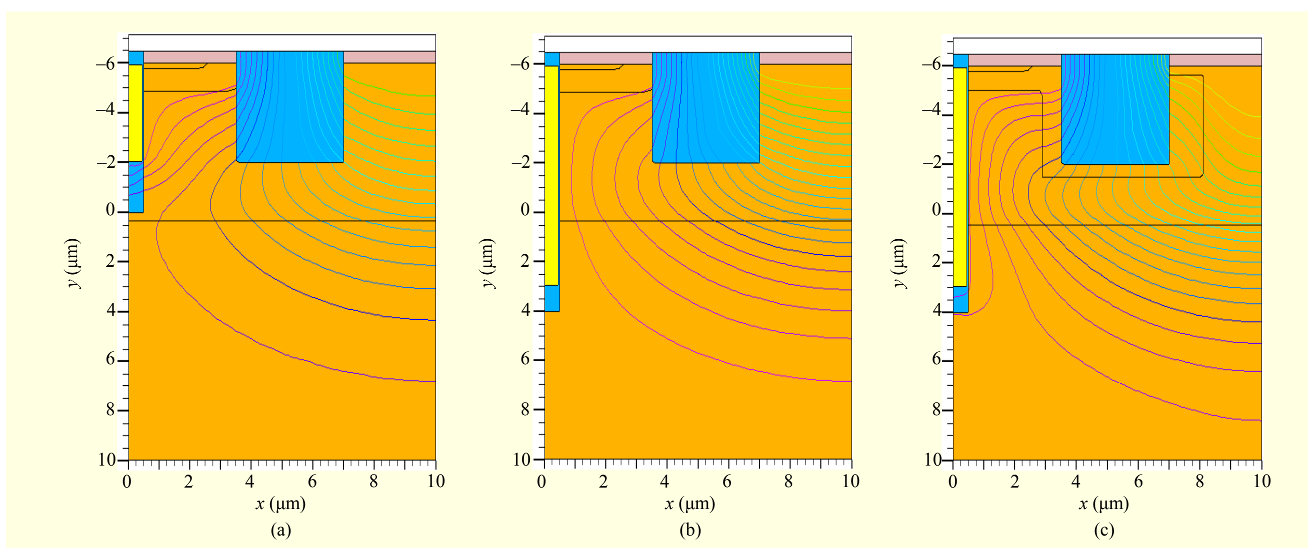

Fig. 4. Equipotential contours at breakdown (10 V/contour) for (a) CTG (201 V), (b) ETG (227 V), and (c) ETGSJ (239 V).

1. Electric Field Distribution

The electric field distribution of each structure (CTG, ETG, and ETGSJ) in three different directions (at breakdown), is shown in Fig. 3. Figure 3(a) depicts the lateral electric field distribution (bulk field) near the thick oxide bottom (y = –1.99, cross section: A-A'). The electric field in the n-drift region is modulated by n- and p-drift junction depletion (Fig. 3(a)). In the ETGSJ structure, unlike in conventional structures, a new electric field peak is generated at the metallurgical junction of the n- and p-drift region. Due to this new peak, electric field modulation occurs, which in turn lowers the peak electric field. Thus, this modulation effect generates a new electric field peak for the newly formed uniform bulk field distribution [6]. The vertical electric field distribution along the sidewall of the trench gate (x = 0.51, cross section: B-B' (in Fig. 2)) is shown in Fig. 3(b), where it can be seen that the electric field peak occurs at the bottom-left corner of the thick oxide and that the ETGSJ structure has a lower electric field peak than that of the CTG structure due to the effect of the electric field modulation that occurs. Figure 3(c) depicts the vertical electric field distribution (x = 9.9, cross section: C-C') along the drain region, where it is evident that the vertical electric field at the drain surface of the ETGSJ is lowered. However, an electric field peak occurs at the n-drift and p-substrate junction due to charge imbalance [10]. The breakdown of the ETGSJ occurs at the p-substrate region in the ETGSJ structure; therefore, the doping concentration of the n-drift and p-substrate should be determined through process simulation.

2. Potential Distribution

The equipotential contours for the three structures — CTG, ETG, and ETGSJ — are depicted in Fig. 4. The electric field in

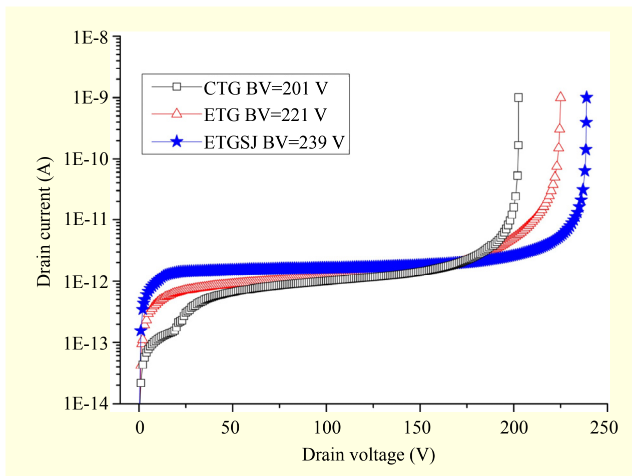

Fig. 5. Forward-blocking I-V characteristics curve at breakdown (V_{GS} = 0 V) for the CTG, ETG, and ETGSJ structures.

the ETGSJ structure is reshaped by the n- and p-drift junction (Fig. 4(c)). Compared to the CTG and ETG structures, the ETGSJ structure shows a relatively high level of doping concentration. This is because the CTG and ETG structures are constrained to having low doping concentrations for the purposes of full depletion. However, as the ETGSJ structure uses the method of junction depletion in the drift, the structure is not constrained by the depth of the junction; hence, a full depletion of the drift is possible while simultaneously maintaining high levels of doping concentration. In addition, the ETGSJ structure is able to sustain high voltages due to having an extended depletion region (in the direction of the lightly doped p-substrate) and a relatively high level of doping concentration compared with that of the CTG and ETG structures. Figure 5 shows the forward-blocking I-V characteristics curve at breakdown for the CTG, ETG, and ETGSJ structures.

Table 1. Performance comparisons of device types.

Device types	BV (V)	$R_{on,sp}$ (mΩ·cm^2)	FOM=BV/$R_{on,sp}$ (V/mΩ·cm^2)
ETGSJ	239	1.05	227.6
ETG	227	1.67	135.9
CTG	201	1.68	119.6
DETG [6]	171	1.31	130.5
SOI DT [7]	233	3.30	70.6
CLAVER LDMOS [11]	150	1.59	94.3

3. Optimization of ETGSJ Structure

For each of the three structures (CTG, ETG, and ETGSJ), Fig. 6 shows the dependency of BV, $R_{on.sp}$, and FOM on drift concentration. As depicted in Fig. 6(a), the CTG and ETG structures' maximum BVs occur at or below $N_D = 3\times10^{15}$ cm^{-3} because their respective n-drift regions are fully depleted. On the other hand, as the ETGSJ structure uses junction depletion, it is fully depleted above $N_{D,A} = 4\times10^{15}$ cm^{-3} — the point at which it yields the overall maximum BV.

The depletion regions in the CTG and ETG structures are of a similar width. However, in the case of the ETGSJ structure, the width of its depletion region is wider in comparison due to the presence of the p-drift. Thus, the ETGSJ structure has a narrower current path in comparison; therefore, it is more likely that the on-resistance of the ETGSJ structure will be high. Even though the ETGSJ structure has a narrower current path, high current density can be obtained by using a higher level of doping concentration in the drift regions. Therefore, as shown in Fig. 6(b), low $R_{on.sp}$ is achieved on account of the fact that the ETGSJ structure has a relatively high level of drift doping

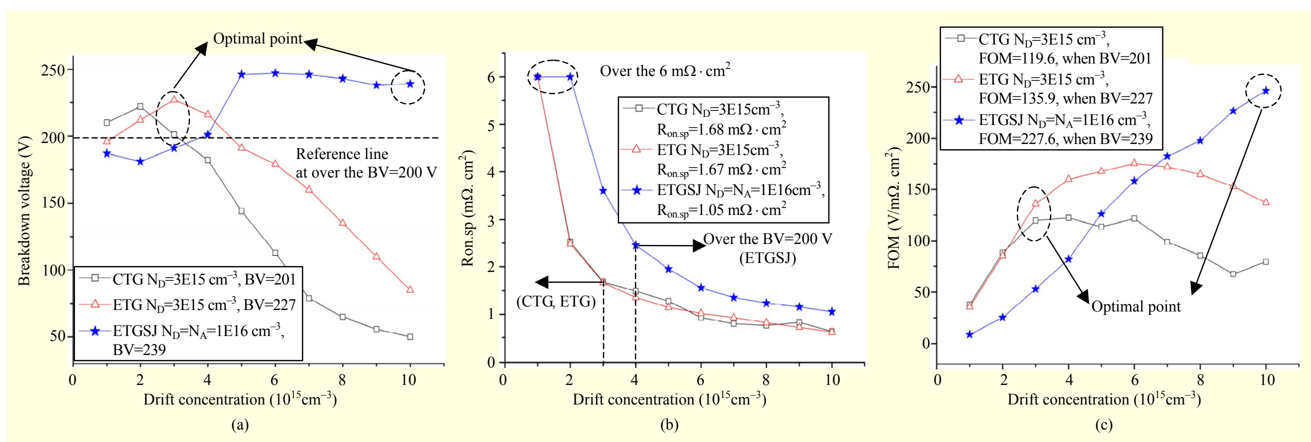

Fig. 6. Dependency of (a) BV, (b) $R_{on.sp}$, and (c) figure of merit (FOM): BV/$R_{on.sp}$ on drift concentration (for CTG, ETG, and ETGSJ structures).

http://dx.doi.org/10.4218/etrij.14.0113.0826

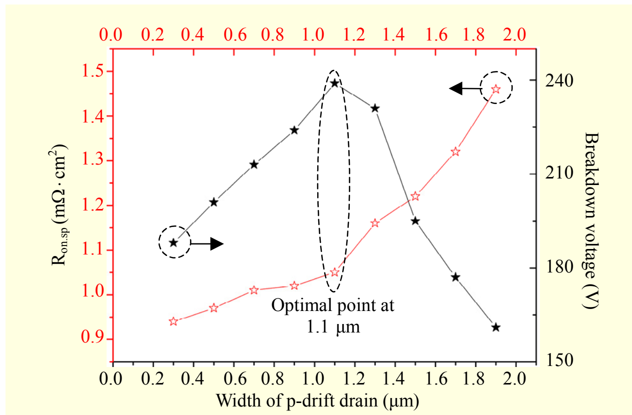

Fig. 7. Optimization of the distance W_pD for maximum V and minimum $R_{on.sp}$.

concentration (optimized at $N_{D,A} = 1\times10^{16}$ cm^{-3}).

As represented in Fig. 6, the ETGSJ structure has relatively high drift doping concentration compared to the other structures and the improvement of $R_{on.sp}$ and FOM is verified. Table 1 shows the performance comparison between the ETGSJ and other structures. The maximum BV of each structure is optimized to be over 200 V for high-voltage applications. Compared to the CTG structure, the results show that the BV of the ETGSJ structure is improved from 201 V to 239 V (16%), while $R_{on.sp}$ is improved from 1.68 mΩ·cm² to 1.05 mΩ·cm² (37.5%).

4. Optimization of Charge Balance in the Drift Region

For the ETGSJ structure, charge balance in the drift region is most important. If a charge imbalance creates a high FOM, as in Fig. 6(c), the ETGSJ structure will not outperform the CTG and ETG structures and will eventually breakdown prematurely. The width of the p-drift region of the p-body side (W_p) and the width of the region beneath the thick oxide are uniformly 0.5 μm. However, the width of the p-drift region of the drain side (W_pD) is 1.1 μm. This is because the hole charge is surplus in the drift region between the p-body and the trench gate. The hole charge flows in at the p-body and the p-substrate through the deep trench gate. On the contrary, the hole charge is lacking in the drain region [6], [10]. As the p-drift width (W_pD) of the drain side has no additionally-induced charge, its width should be wider than W_p or it should have a higher level of doping concentration [6]–[7]. As a result, optimal charge balance with high performance is only achievable when W_pD is 1.1 μm, as shown in Fig. 7.

IV. Conclusion

In this paper, the ETGSJ structure with the improved silicon limit of power MOSFET is proposed. Because of the charge balance effect, the BV and $R_{on.sp}$ are improved while simultaneously maintaining a high level of doping concentration. The experimental results show that the BV and $R_{on.sp}$ are improved by 16% and 37.5%, respectively, compared to the CTG structure.

References

[1] K.R. Varadarajan, A. Sinkar, and T.P. Chow, "Novel Integrable 80 V Silicon Lateral Trench Power MOSFETs for High Frequency DC–DC Converters," *Power Electron. Specialists Conf.*, Orlando, FL, USA, June 17–21, 2007, pp. 1013–1017.

[2] W.S. Son, Y.H. Sohn, and S.Y. Choi, "RESURF LDMOSFET with a Trench for SOI Power Integrated Circuits," *Microelectron. J.*, vol. 35, no. 5, May 2004, pp. 393–400.

[3] N. Fujishima and C.A.T. Salama, "A Trench Lateral Power MOSFET Using Self-Aligned Trench Bottom Contact Holes," *Electron Devices Meeting,* Washington, DC, USA, Dec. 10, 1997, pp. 359–362.

[4] K.R. Varadarajan et al., "250 V Integrable Silicon Lateral Trench Power MOSFETs with Superior Specific on-Resistance," *Power Int. Symp. Semicond. Devices IC's,* Jeju, Rep. of Korea, May 27–31, 2007, pp. 233–236.

[5] B.J. Baliga, *Fundamentals of Power Semiconductor Devices*, 1st ed., New York: Springer, 2008.

[6] L. Yue, B. Zhang, and Z. Li, "A Lateral Power MOSFET with the Double Extended Trench Gate," *IEEE Electron Device Lett.*, vol. 33, no. 8, Aug. 2012, pp. 1174–1176.

[7] X. Luo et al., "Ultralow Specific on-Resistance High-Voltage SOI Lateral MOSFET," *IEEE Electron Device Lett.*, vol. 32, no. 2, Feb. 2011, pp. 185–187.

[8] B. Zhang et al., "High-Voltage LDMOS with Charge-Balanced Surface Low on-Resistance Path Layer," *IEEE Electron Device Lett.*, vol. 30, no. 8, Aug. 2009, pp. 849–851.

[9] Silvaco, Inc., *Atlas User's Manual: Device Simulation Software*, Santa Clara, CA, USA: Silvaco, Inc., 2008.

[10] H. Wang, E. Napoli, and F. Udrea, "Breakdown Voltage for Superjunction Power Devices with Charge Imbalance: An Analytical Model Valid for Both Punch through and non Punch through Devices," *IEEE Trans. Electron Devices,* vol. 56, no. 12, Dec. 2009, pp. 3175–3183.

[11] T. Khan et al., "Combined Lateral Vertical RESURF (CLAVER) LDMOS Structure," *Power Semicond. Devices IC's,* Barcelona, Spain, June 14–18, 2009, pp. 13–16.

Doohyung Cho received his BS degree in electrical and electronic engineering from Dankook University, Seoul, Rep. of Korea, in 2011 and his MS degree in electronic engineering from Sogang University, Seoul, Rep. of Korea, in 2013. He is currently working toward his PhD in electronic engineering at Sogang University. His main research interests are focused on Si/SiC power semiconductor devices and power conversion circuits.

Kwangsoo Kim received his BS, MS, and PhD degrees in electronic engineering from Sogang University, Seoul, Rep. of Korea, in 1981, 1983, and 1992, respectively. From 1992 to 1997, he was with the Electronics and Telecommunications Research Institute working on silicon devices (CMOS, Bipolar & BiCMOS). From 1988 to 1992, he carried out his PhD dissertation on the high-speed and high-density BiCMOS device while at Sogang University. From 1999 to 2005, he was a principal research engineer at the Institute for Information Technology Advancement, Daejeon, Rep. of Korea, where he planned new component technology about Information & Communication Technology of Korea. From 2005 to 2008, he was a principal research engineer with Daegu Gyeongbuk Institute of Science and Technology, Daegu, Rep. of Korea, where he conducted research on IT convergence technology for intelligent vehicles. He joined Sogang University in 2008. His current research interests are the technology, modeling, and reliability of semiconductor devices; especially power devices.

http://dx.doi.org/10.4218/etrij.14.0113.0826